The Permian-Triassic Boundary in the Carnic Alps of Austria (Gartnerkofel Region)			Editors: W.T. Holser & H.P. Schönlaub	
Abh. Geol. B.-A.	ISSN 0378-0864 ISBN 3-900312-74-5	Band **45**	S. 37–51	Wien, Mai 1991

The Permian-Triassic of the Gartnerkofel-1 Core (Carnic Alps, Austria): Petrography and Geochemistry of an Anisian Ash-Flow Tuff

By JOHANNES H. OBENHOLZNER*)

With 10 Text-Figures, 4 Tables and 2 Plates

Carinthia
Carnic Alps
Anisian
Ash-flow tuff
Petrography
Geochemistry
Alteration

Österreichische Karte 1 : 50.000
Blatt 198

Contents

Zusammenfassung

In der Forschungsbohrung Gartnerkofel-1 am Naßfeld in den Karnischen Alpen wurde zwischen 30 und 34,5 m eine Lage von dazitischem Aschentuff erbohrt, der sich dem fluviatil gebildeten Muschelkalkkonglomerat zwischenschaltet. Der Tuff ist gering verschweißt und alle Glasscherben sind devitrifiziert und umgewandelt. Die Geochemie nach Haupt-, Spuren- und SE-Elementen zeigt charakteristische Verteilungsmuster und Verhältniswerte, die einem „orogenen", kalkalkalischen Magmentyp entsprechen.

Abstract

The drilling project Gartnerkofel-I discovered between 30 and 34.5 m a layer of dacitic ash-flow tuff within a fluvial conglomerate sequence (Anisian Muschelkalk Conglomerate). The tuff is slightly to moderately welded and all glass shards are devitrified and altered. Bulk rock geochemistry of main, trace and RE elements show characteristic element contents and ratios of an "orogenic", calcalkaline magma.

1. Introduction

The Middle Triassic magmatism is an igneous event settled between Variscean and Alpine orogeny. In the Southern Alps this event is documented by intrusives, lavas, pyroclastic rocks and volcanogenic sediments from Scythian to Carnian times. The studied ash-flow tuff is the only pyroclastic deposit known from the Anisian. During the Ladinian, ignimbrites covered large areas in the eastern part of the Southern Alps, but nowadays these rocks are hardly exposed. So the drilling project Gartnerkofel-I enabled us for the first time

*) Author's address: Dr. JOHANNES H. OBENHOLZNER; Institut für Geowissenschaften; Montanuniversität Leoben; Franz-Josef-Straße 18; A-8700 Leoben.

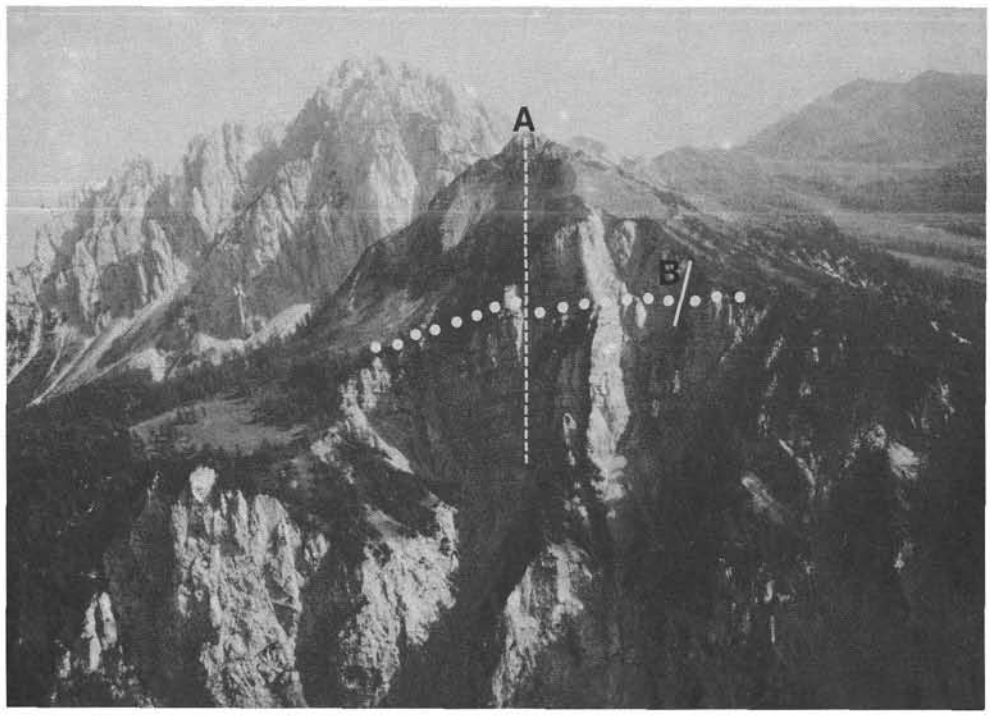

Text-Fig. 1.
Aerial photograph from the north of the Reppwand with the Gartnerkofel (2195 m) in the background.
A: Drill site on Kammleiten (1998 m);
B: Top of the outcrop section.
Dotted line indicates the Permian–Triassic boundary between the Bellerophon Formation (below) and the Werfen Formation above.
Photo: G. FLAJS, Aachen.

to examine a whole section of a Middle Triassic ash-flow tuff.

A 4-m drilling core and a small outcrop have been at our disposal to investigate this pyroclastic deposit, which is otherwise totally covered by sediments or hidden by Alpine tectonics. It is obvious that these poor possibilities of observation are not enough to solve all volcanological problems, so some of the results are hypothetical but help to elucidate the physiology of one of the ignimbrites in the Alpine area.

2. Geological Setting

(Text.Fig. 1)

The basal conglomerate, the ash-flow tuff (AFT, according to ash particle grain size) and the upper conglomerate are also exposed at an outcrop, where the AFT is only about 1 m thick and strongly tectonized (F. KAHLER & S. PREY, 1963). The core brought up rather fresh material and shows a section of 4 m through a macroscopically homogeneous layer, which is covered by a 10-cm-thick volcaniclastic bed. This reworked co-ignimbritic ash-fall deposit contains rare clasts of the AFT. The AFT at the outcrop and at the core, separated only about 30 m, represents the distal facies of a pyroclastic deposit. The decrease of thickness from E to W could be depositional due to morphology or perhaps indicates a flow direction (the massive Ladinian carbonate build up of the Gartnerkofel presently covers the possible source area).

The top of the lower conglomerate does not show any contact features (like reddening) at its boundary with the AFT, nor have fiamme structures been observed. The upper conglomerate contains boulders of the AFT as well as volcanic pebbles of different origin, indicating that the source area was eroded shortly after deposition of the pyroclastic cloud. No time equivalent, terrestric sediments or volcanics are known in the entire area of the Carnic Alps, so it is not possible to correlate this pyroclastic event to an on-land volcanic terrain or to a caldera structure. The sediments below and above the conglomerate sequence are marine.

The core is slightly tectonized at its base and top. From 30 to 32 m the colour of this rock is red, from 32 to 33 m there is a transition zone from red to green and the base is gray-green (see Text-Fig. 2). This indicates differing oxidation and reduction conditions through the AFT. The famous ash-flow tuff of the Capel Curig Formation (Wales) shows similar features, which have been interpreted as a partially subaqeous, partially subaerial deposition and alteration (M.F. HOWELLS et al., 1979).

The whole sequence (fluvial conglomerates according to M. SCHMIDT (1987) and ash-flow tuff) documents an emersion phase of a hinterland in the Triassic (P. CROS, 1982), which is represented in the Austrian part of the Carnic Alps only by marine sediments (limestones, dolomites, shales). The Anisian conglomerates can be traced also to the Italian part of the Carnia, for instance to the Val Canale (Ugovizza Breccia: E. FARABEGOLI et al., 1985), but lacks any beds of pyroclastic rocks or lavas. Very rarely does the Ugovizza Breccia contain boulders of lava and tuffitic groundmass.

3. Petrography

All glass shards, constituting the matrix up to 60 % to 70 % of volume, are devitrified and altered to varying degrees. The shapes of the slightly elongated shards are outlined by iron oxides (Plate 2, Fig. 4). These features are best preserved in the upper, reddened part of the layer (rich in fine scattered iron oxides; greenish part is rich in chlorite). Below single crystals and microxenoliths, typical matrix deformation caused by load compaction of the AFT, can be observed. The shards consist of quartz and K-feldspar and are partially replaced by carbonate and/or clay minerals.

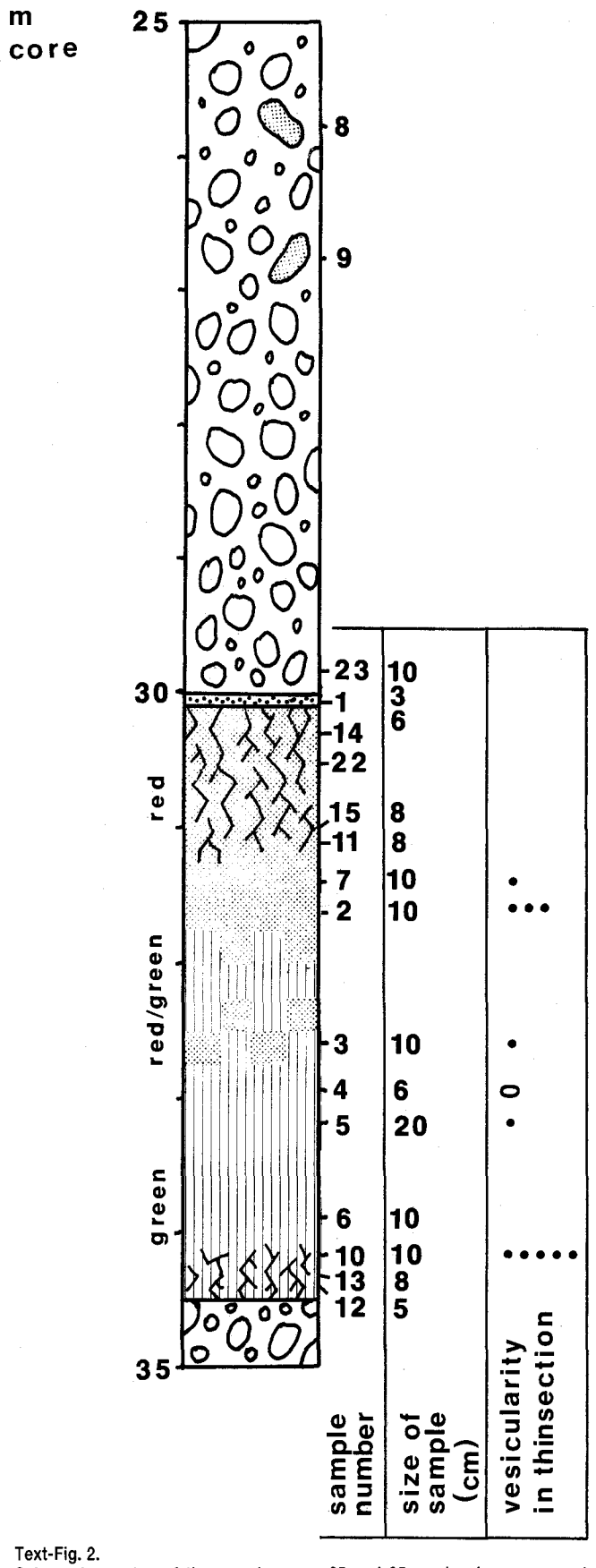

Text-Fig. 2.
Schematic section of the core between 25 and 35 m, showing uppermost top of lower conglomerate, ash-flow tuff layer, and ash-flow tuff boulder containing upper conglomerate.
Dot pattern signifies red color; line pattern gray-green. The vesicularity in thinsection is indicated by points per vacuole. Sample no. 6 shows one larger vacuole (diameter 2.5 cm).

The tectonization and alteration at the base and at the top do not allow one to estimate the degree of welding relative to the central part (31.3–33.94 m), which is slightly to moderately welded. All shard textures in the tectonized parts of the core are either "ghost"-like, or destroyed.

The only partially fresh component is intermediate plagioclase (10 %–15 % of volume), which is often embayed and zoned (for mineral chemistry, see Table 2). In the Or-Ab-An triangle most of the analyses plot in the andesine field; a few crystals have oligoclase or labradorite composition. Sometimes crystal clots of plagioclase can be observed, but in general plagioclase occurs as individual pheno- or xenocrysts in the matrix (Plate 2, Fig. 3; Plate 2, Fig. 4).

A second type of plagioclase shows poikilitic inclusions of glass droplets (now chlorite as an alteration product of a basic to intermediate glass composition).

The association of poikitlitic and inclusion-free plagioclases is also known from Upper Anisian andesitic and dacitic lavas from the Karawanken Mountains (J.H. OBENHOLZNER, 1984). There the poikilitic ones are interpreted to be a petrographic indication for magma mixing. The example from the AFT (Plate 2, Fig. 2) shows a deep resorption embayment, significant for disequilibrium between crystal and melt. As we found no other indications for mixing, it is not provable; but magma mixing can be an important factor in triggering explosive eruptions (S.R.J. SPARKS et al., 1977).

The poikilitic plagioclases may also represent the product of an earlier eruption. These crystals might have been picked up during emplacement of the AFT.

Chlorite pseudomorphs after clinopyroxene(?), pumice fragments (0.3–1.2 mm) and microxenoliths of andesitic lava (Plate 2, Fig. 1), arenite (Werfen Formation?) and an older welded ash-flow tuff are rare and scattered in the core. It is very common to find lava fragments, of a composition more basic than the juvenile components, reworked in a pyroclastic deposit (C.S. ROSS & R.L. SMITH, 1961).

Accessories are altered Ti-magnetite, sometimes embayed, now consisting of an intergrowth of ilmenite and hematite (both in the red and green part), and apatite.

Two types of pumice fragments can be distinguished. One type is angular, white, with tubular, wormlike vesicles, sometimes containing larger ovoid vesicles. This pumice is considered to be a lithic, maybe more silicic component (Plate 1, Fig. 1). The other pumice type shows brownish colours, identical with the AFT but slightly deformed, with tubular vesicles only; representing a juvenile component (Plate 1, Fig. 2).

Irregularly shaped gas vacuoles with average diameter of 1 cm are common, but do not show a systematic distribution from base to top with lowest abundance in the central part as would be expected (C.S. ROSS & R.L. SMITH, 1961). This could be of restricted sampling by the core. The vacuoles are zonally filled with chlorite, carbonate minerals or quartz (Plate 1, Fig. 3).

X-ray diffractometry of the AFT boulders, which do not contain any primary minerals (except ore-phenocrysts and apatite), showed that palygorskite, a K-rich montmorillonite (?) and hematite build up this rock, which still exhibits the AFT texture in thin section. X-ray diffractometry had been done by E. KIRCHNER. A detailed study of alteration minerals is in preparation.

Table 1.
Frequency of crystals and xenoliths.

	[%]	Size [mm]	Shape
Intermediate plagioclase	10–15	0.3–3	pheno- to xenocryst; often embayed
Pseudomorphs (CHL after CPX ?)	1	0.9–1	pheno- to xenocryst
Ore	1	0.15–0.5	pheno- to xenocryst
Vacuoles	1–2	0.5–20	irregular
Welded tuff fragments	2	0.12–0.3	lensoid to angular
Pumice	4–8	0.3–1.2	lensoid to angular
Andesitic lava fragments	2	0.9–1.5	subangular
Arenite	2	0.6–2.4	slightly rounded
Crystal clots	<1	0.3–1.2	irregular
Carbonate xenolith	<1	4.5	slightly rounded
Matrix (shards)	60–70	0.1–0.25	plate-, shred-like

The AFT boulder (Sample 9) includes a dolomite clast, which shows a 2-mm-thick, pale green contact rim of chlorite and minor amounts of talc. This indicates that dolomitization – or at least an early phase of dolomitization – occured prior to the eruption of the AFT.

4. Geochemistry

Bulk rock geochemistry was analyzed. Even such an analysis for ash-flow tuffs is rather unusual (R.A.F. CAS & J.V. WRIGHT, p. 258–260, 1987). But the absence of fresh glass or magma characterizing minerals led us to test the chemical composition of several segments of the core that are macroscopically homogeneous, vesicle free and do not contain xenoliths larger than 1 mm.

Eleven samples from the ash-flow tuff, 1 sample from the ash tuffite (clast-free, homogeneous material) and 4 boulders (2 AFT, 2 non-AFT boulders) of the upper conglomerate were analysed to demonstrate alteration effects and to define a possible original magma composition.

The two non-AFT boulders are strongly altered ash-flow tuff clasts from the upper conglomerate outcrop near the drilling site, which do not correlate petrographically with the AFT event. They had been analyzed together with 4 Ladinian ash-flow tuff samples from Italy and Yugoslavia to figure out if there exists a geochemical relation or evolution between these Middle Triassic pyroclastic events.

Analyses were done by XRAL, Ontario for main and selected trace elements (Sr, Rb, Cr, Zr, Nb, Y, Ba) X-Ray Fluorescence Spectrometry and by C.J. ORTH, Los Alamos for REE, Th, Ta, Hf and U by Neutron Activation Analysis.

Table 2.
Mineralchemistry of plagioclases (selected microprobe analyses).
Analyst: G. NEUHUBER; Institute of Geosciences, Salzburg University.
Pl = plagioclase; c = core; r = rim; mp = middle part.

	Sample No. 2			Sample No. 5				Sample No. 10				
	Pl 4.1c	Pl 5.1c	Pl 5.2r	Pl 4.1r	Pl 5.1mp	Pl 5.2mp	Pl 2.1r	Pl 1.1mp	Pl2.3mp	Pl3.1mp	Pl4.2c	Pl4.3mp
SiO_2	57.4	58.54	58.72	57.37	58.55	58.72	55.95	58.42	59.2	58.83	59.3	59.71
Al_2O_3	26.42	25.79	25.5	26.42	25.79	25.5	27.69	26.42	26.83	25.73	25.95	26.08
CaO	9.4	8.7	8.58	9.4	8.7	8.58	11.63	7.4	5.2	7.3	6.4	6.42
Na_2O	6.25	6.31	6.46	6.25	6.31	6.46	4.9	6.69	7.54	6.3	6.91	6.85
K_2O	0.62	0.73	0.83	0.62	0.73	0.83	0.24	1.04	1.32	1.3	1.31	1.14
BaO	0.0	0.0	0.0	0.0	0.0	0.0	0.0	0.04	0.05	0.06	0.12	0.12
Σ	100.09	100.07	100.09	100.06	100.08	100.09	100.41	100.01	100.14	99.52	99.99	100.32
Si	10.316	10.489	10.526	10.314	10.49	10.526	10.045	10.464	10.549	10.58	10.605	10.625
Al	5.598	5.448	5.389	5.6	5.447	5.389	5.861	5.579	5.636	5.455	5.471	5.471
Ca	1.81	1.67	1.684	1.811	1.67	1.648	2.237	1.42	0.993	1.407	1.226	1.224
Na	2.178	2.192	2.245	2.179	2.192	2.245	1.706	2.323	2.605	2.197	2.396	2.363
K	0.142	0.167	0.19	0.142	0.167	0.19	0.055	0.237	0.3	0.298	0.299	0.259
Ba	0.0	0.0	0.0	0.0	0.0	0.0	0.0	0.003	0.003	0.004	0.008	0.008
Or	3.5	4.1	4.6	3.5	4.1	4.6	1.4	6.0	8.0	7.7	7.3	7.4
Ab	52.7	54.4	55.0	52.7	54.4	55.0	42.6	58.3	67.2	56.3	60.7	60.0
An	43.8	41.5	40.4	43.8	41.5	40.4	56.0	35.7	24.8	36.0	32.0	32.6

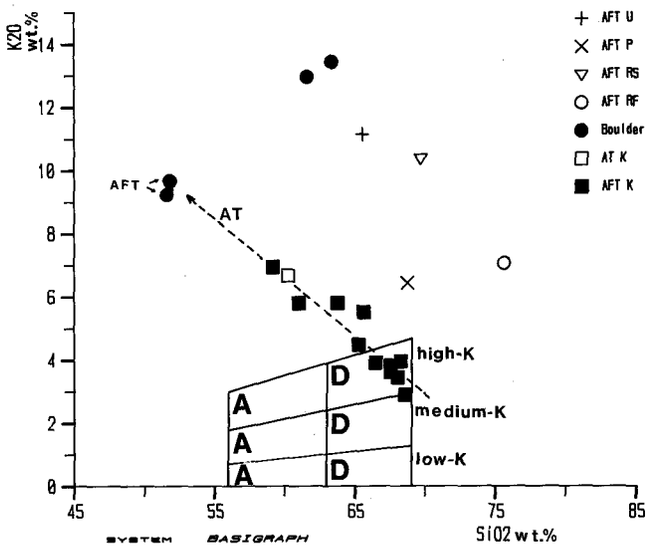

Text-Fig. 3.
Partial reproduction of the K_2O-SiO_2 classification diagram for magmatic rocks after EWART (1979).
AFT U = Ash-flow tuff Ugovizza (Italy); AFT P = Ash-flow tuff Podlog (Yugoslavia); AFT RS = Ash-flow tuff Rio Salto (Italy); AFT RF = Ash-flow tuff Rio Freddo (Italy); AT K = Ash tuffite Kammleiten; AFT K = Ash-flow tuff Kammleiten. Volcanic boulders from the upper conglomerate are indicated by solid circles; AFT-boulders are indicated by "AFT" and arrows. A = High-K Andesite; D = High-K Dacite; AT = Alteration trend.
For main element plots only as LOI free recalculated values are used.

4.1. Main Element Geochemistry

The samples from the central part are of high-K-dacitic composition (Text-Fig. 3). The discrimination fields for andesites and dacites refer to A. EWART (1979). In the K_2O-SiO_2 diagram, an alteration trend (AT) is evident, showing for the samples from the base and the top and for the 2 AFT boulders strong K_2O enrichment and SiO_2 depletion. Reference samples of the non-AFT boulders and of lower Ladinian AFTs and ignimbrites from the eastern part of the Southern Alps (AFT-U, AFT-P, AFT-RS, AFT-RF) are clearly of even higher K_2O contents and partially of higher SiO_2 contents than typical AFT samples from the central part of the core.

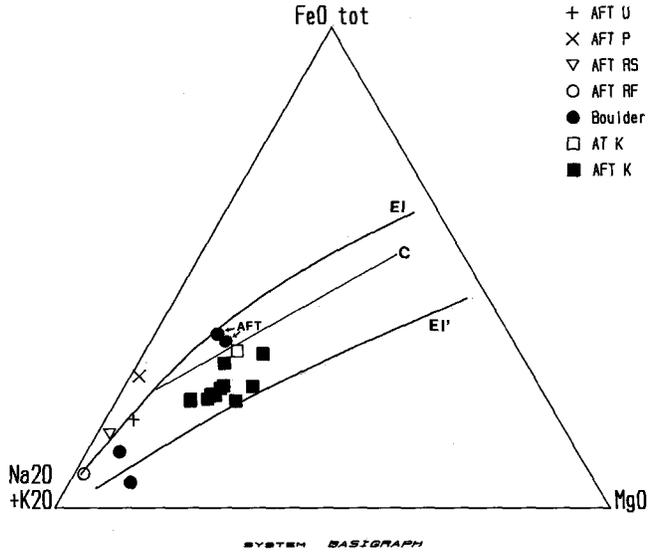

Text-Fig. 4.
AFM Diagram.
Symbols as in Text-Fig. 2.
C = Calcalkaline trend of Cascades (USA). EI – EI' = Field for calcalkaline volcanics of Eolian Islands (Italy).

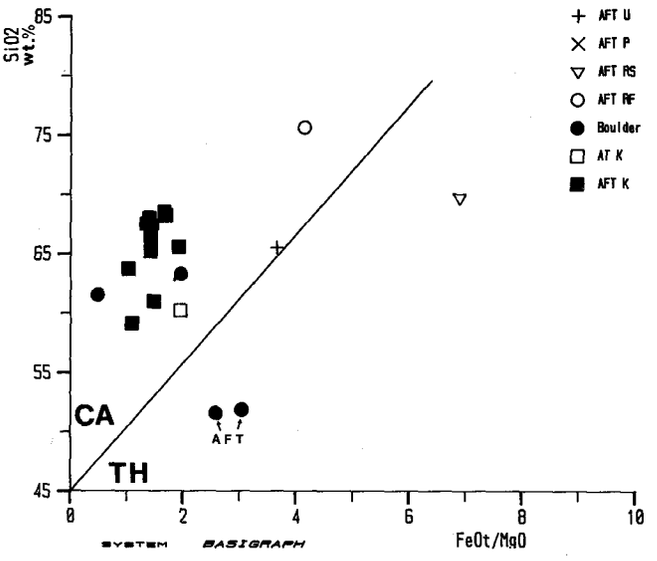

Text-Fig. 5.
SiO_2-FeO_{tot}/MgO Diagram.
CA = Calcalkaline field; TH = Tholeiitic field.
Symbols as in Text-Fig. 2.

It seems that the reference samples had also been affected by a secondary K influx, which can be seen for many Triassic volcanics of the Southern Alps. An enrichment factor up to 3 had been observed (P. SPADEA, 1970; F. LUCCHINI et al., 1980; G. DE VECCHI & V. DE ZANCHE, 1982; J.H. OBENHOLZNER, 1984). This kind of metasomatism often described from intracontinentally erupted lavas is still problematical to explain (D. SAWYER et al., 1989). Most of the cited authors consider a hydrothermal activity to be responsible for this phenomenon.

It is interesting to remark that for all AFT samples the sum $Na_2O + K_2O$ is nearly constant (6.6–7.5). This indicates a successive exchange of bulk rock Na by K, mostly effecting the plagioclase phases by replacing the albit component by orthoclase(?). Such hetero-

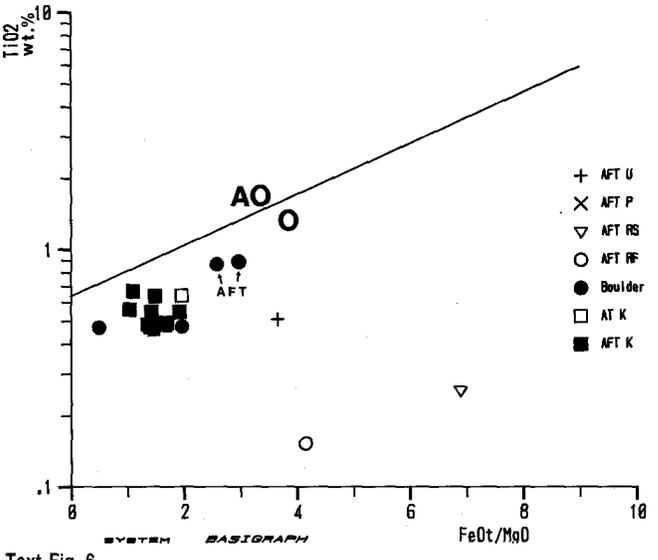

Text-Fig. 6.
TiO_2-FeO_{tot}/MgO Diagram.
AO = Anorogenic field; O = Orogenic field.
Symbols as in Text-Fig. 2.

geneous feldspars are also known from other Triassic volcanic rocks in the Southern Alps (J.H. OBENHOLZNER, 1984; P.L. ROSSI et al., 1979).

In the AFM diagram all samples of the AFT, including the two AFT boulders, plot within the area of calcalkaline rocks. The reference samples and the two non AFT boulders are more alkaline (Text-Fig. 4).

In the SiO_2-FeO_{tot}/MgO diagram (A. MIYASHIRO, 1974; Text-Fig. 5) all samples plot within the field of calcalkaline rocks, except the two AFT boulders and AFT-RS and AFT-P (out of diagram range). The AFT boulders are strongly altered and enriched in FeO_{tot}. Alteration effects are discussed below. The geochemical characterization of the reference samples outlines a higher FeO_{tot}/MgO ratio than the AFT samples.

In the TiO_2-FeO_{tot}/MgO diagram (J. BEBIEN, 1980; Text-Fig. 6) all samples plot within the field of orogenic rocks (AFT-P is out of diagram range).

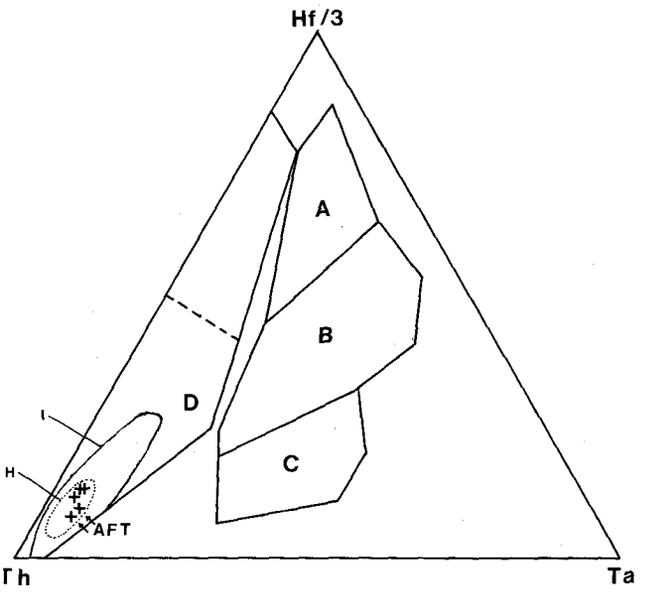

Text-Fig. 7.
Hf/3-Th-Ta Diagram.
A = N-type MORB; B = E-type MORB and tholeiitic within-plate basalts and differentiates; C = Alkaline within-plate basalts and differentiates; D = Convergent plate-margin basalts and differentiates - calcalkaline rocks plot in the Th-rich part of field D; H = Samples from Hungary; see text; I = Samples from Italy; see text.

4.2. Trace Element Geochemistry

The high-K-dacitic composition of the AFT is verified by the SiO_2-Nb/Y diagram (not shown; J.A. WINCHESTER & P.A. FLOYD, 1977). Only strongly altered samples and the rhyolitic AFT-RF plot outside the dacitic field.

The Nb-SiO_2 diagram (not shown; J.A. PEARCE & G.H. GALE, 1977) indicates that all samples are orogenic, except the two strongly altered AFT-boulders.

The plate tectonic interpretation of the cited diagrams is also in agreement with the Hf/3-Th-Ta plot (D.A. WOOD et al., 1979; Text-Fig. 7). This diagram, which was designed especially for basalts and their differentiates from various tectonic settings, demonstrates that 3 of the AFT samples and the 2 AFT boulders plot within the field (D) of magmas from convergent plate margins. This diagram shows also the fields for Middle Triassic lavas from the Buda Mountains, Hungary (H: data from E. HORVATH & G. TARI, 1987) and the Dolomites, northern Italy (I: data from CASTELLARIN et al., 1988); which enclose the area of the AFT plots.

It is necessary to mention that the Hf and Th and to a lesser degree the Ta contents of the boulders are higher than the contents of the AFT samples.

Table 3.
Main and trace element data of AFT (no. 1–15); B1(9) = AFT boulder; B3(16), B4(17) = non-AFT boulders. Reference samples of Ladinian ash-flow tuffs from the eastern Southern Alps (RF = Rio Freddo (Italy); RS = Rio Salto (Italy); P = Podlog (Yugoslavia); U = Ugovizza (Italy).

S.No.	Depth	SiO_2	TiO_2	Al_2O_3	Fe_2O_3	MnO	MgO	CaO	Na_2O	K_2O	P_2O_5	LOI	SUM	Cr	Rb	Sr	Y	Zr	Nb	Ba
1	30.2	56.3	0.6	20.2	5.49	0.02	2.52	0.57	1.44	6.23	0.04	6.39	99.8	19	127	55	64	461	31	85
15	31.14	56.4	0.59	18.6	5.29	0.02	3.2	1.3	1.52	5.36	0.11	7.47	99.86	15	133	75	63	451	33	293
11	31.2	62.3	0.52	16.5	4.58	0.01	2.14	1.34	2.21	5.23	0.1	5.16	100.09	17	113	97	44	394	26	290
7	31.4	65.4	0.46	14.8	2.74	0.03	1.48	3.18	4.39	2.75	0.09	4.7	100.02	12	66	124	29	346	26	365
2	31.5	65.1	0.47	15.2	2.79	0.02	1.48	3.0	3.4	3.77	0.09	4.7	100.02	14	76	98	42	339	19	231
3	32.7	62.0	0.52	16.4	3.67	0.02	2.32	2.56	3.14	4.25	0.1	4.93	99.91	12	88	115	57	395	10	412
4	33.0	62.6	0.48	15.0	3.26	0.03	2.06	3.82	3.12	3.67	0.1	5.7	99.84	10	92	95	48	344	22	210
5	33.12	64.8	0.45	14.9	2.87	0.03	1.85	3.26	3.67	3.27	0.09	4.77	99.96	15	77	107	55	342	16	272
6	33.8	64.0	0.46	14.9	2.87	0.03	1.92	3.86	2.95	3.61	0.1	5.47	100.17	12	86	110	52	338	10	175
10	34.2	63.8	0.44	14.5	2.98	0.03	1.88	3.80	3.46	3.41	0.09	5.31	99.7	14	84	114	50	317	15	232
13	34.3	59.2	0.52	17.6	3.12	0.02	2.72	2.42	1.72	5.38	0.1	6.77	99.57	12	139	79	38	413	26	246
12	34.4	53.9	0.61	19.6	4.09	0.01	3.38	1.82	1.21	6.32	0.11	8.39	99.44	16	163	63	56	438	27	285
B1(8)	25.8	48.4	0.82	25.2	6.94	0.01	2.07	0.5	0.13	8.94	0.1	7.23	100.34	13	146	10	17	365	39	157
B2(9)	26.8	47.6	0.8	25.8	6.41	0.01	2,24	0.6	0.09	8.52	0.1	8.23	100.4	11	163	10	25	455	32	109
B3(16)	-	61.3	0.46	16.8	2.16	0.01	0.99	1.19	0.72	13.0	0.11	2.39	99.13	10	197	16	25	325	13	344
B4(17)	-	57.5	0.44	16.1	0.93	0.01	1.72	3.51	0.91	12.1	0.11	4.93	98.26	10	216	163	34	290	17	3830
RF(18)	-	74.3	0.15	12.7	0.83	0.01	0.18	0.34	2.7	6.93	0.03	0.85	99.02	10	193	10	41	189	29	166
RS(19)	-	68.6	0.25	14.8	2.45	0.02	0.32	0.11	1.55	10.2	0.05	0.77	99.12	10	179	11	80	255	10	499
P(20)	-	68.2	0.43	15.0	4.32	0.03	0.22	0.77	3.7	6.37	0.09	0.85	99.98	13	229	103	46	363	27	775
U(21)	-	63.0	0.49	15.7	3.21	0.01	0.79	0.83	1.29	10.7	0.08	2.93	99.03	10	195	24	45	304	20	340

Table 4.
RE and trace element data of AFT.

Sample No.	Depth	La	Ce	Nd	Sm	Eu	Tb	Dy	Yb	Lu	Hf	Ta	Th	U
15*)	31.14	36	71	27	6.1	0.78	0.79	5.0	2.53	0.32	5.4	0.68	13.3	1.75
11*)	31.2	39	73	37	6.7	0.85	0.76	5.0	2.48	0.35	6.6	0.76	14.8	3.71
7	31.4	54	107	55	9.5	1.14	1.08	6.9	3.6	0.57	9.5	1.12	20.5	5.5
2	31.5	50	101	43	8.9	1.06	0.87	6.9	3.9	0.53	8.2	0.55	19.2	5.2
10	34.2	51	104	45	8.9	1.09	1.05	7.3	4.4	0.6	8.6	0.97	21.1	5.5
13*)	34.3	32.2	53	20	5.1	0.62	0.51	4.1	2.22	0.28	4.6	0.55	10.5	3.29
12*)	34.4	40	78	37	6.7	0.78	0.74	5.1	2.8	0.35	6.9	0.77	15.9	4.22
B1(8)	25.8	11	24	12	3.17	0.53	0.57	4.5	1.6	0.26	11.3	1.85	38.0	2.06
B2(9)	26.8	22	40	30	5.7	0.67	0.66	5.2	1.8	0.22	12.8	1.71	33.9	1.75
B3(16)*)	—	19.3	40.6	17	3.96	0.42	0.43	2.9	1.73	0.21	5.0	0.65	12.6	2.60
B4(17)*)	—	26.9	59	30	5.8	0.77	0.84	5.1	2.8	0.41	9.3	1.24	22.4	5.18
RF(18)*)	—	50	90	39	8.0	0.34	0.89	6.4	4.2	0.53	5.9	0.79	19.3	3.9
RS(19)*)	—	64	132	50	11.3	0.75	1.62	10.9	6.0	0.81	7.1	1.06	22.5	4.84
P(20)*)	—	54	106	50	8.7	1.11	1.01	6.7	4.5	0.61	9.5	1.07	22.1	5.34
U(21)*)	—	50	105	44	9.2	1.25	1.00	6.0	4.4	0.59	9.4	1.11	21.4	8.78

*) Analyses of indicated samples arrived after deadline for the manuscript and are not shown in the diagrams.
The AFT samples (11, 12, 13, 15) from the base and from the top of the pyroclastic deposit show same REE patterns as the samples from the cantral part of the AFT, but are shifted downwards, as it was expected from the REE distribution of the two AFT boulders [B1(8), B2(9)]. See also Text-Fig. 10.
All additional analyses plot in the Hf/3-Th-Ta diagram at the Th-rich corner (field D) close to the samples shown in Text-Fig. 9.
The La/Th ratios are 2 to 4; exceptions are the non-AFT boulders [B3(16), B4(17): La/Th = less than 2].

4.3. REE Characteristics

Results of S. KOSHIMIZU (1984), who demonstrated that REE contents of glass separates and bulk rock analysis of pyroclastic-flow deposits are very close (except Eu contents), encouraged the author to test the REE contents of 7 AFT, 2 AFT boulder and 2 non-AFT boulder samples.

Text-Fig. 8 shows a rock/chondrite diagram (average chondrite after N. NAKAMURA, 1974) for 3 AFT samples from the central part and the 2 AFT boulders (4 REE analyses from the base and the top show identical patterns; not drawn in Text-Fig. 8).

The two indicated fields for rift-related anorogenic andesites (RRAA) and high-K-orogenic andesites (HKOA) are taken from J. GILL (1981) and do not represent discrimination fields, but demonstrate the difference in rock/chondrite ratios for REEs between the two distinct tectonic settings. Samples 2, 7 and 10 are relatively fresh parts of the core showing a slight enrichment of light REEs compared with typical rock/chondrite ratios of high-K-intermediate, orogenic rocks and a negative Eu anomaly, which is expected for samples more acidic than typical andesites (plagioclase fractionation?).

The pattern of the AFT boulders (Samples 8 and 9) is shifted downwards, without remarable pattern change, indicating no selective REE mobility. Similar REE behaviour had been described for altered basalts (P.L. HELLMAN et al., 1979).

For comparison, an Andean dacite (R.S. THORPE et al., 1976; DA) is drawn, showing lower rock/chondrite ratios than the relatively fresh AFT samples and a smaller negative Eu anomaly. Two dacites (64.17 % and 67.04 % SiO_2) from the Rio Grande Rift (USA) have same light REE contents but steeper slopes and no Eu anomaly (data from M.A. DUNGAN et al., 1989; not drawn in Text-Fig. 8).

The La/Nb (2–5) and La/Th ratios (2–7) are typical for high-K-intermediate, orogenic rocks (J. GILL, 1981).

5. Alteration

For estimating the natural element variability respectively secondary mobility. Text-Fig. 9 shows the ratio of rock to the least altered sample (no. 7 is considered as a nearly relict domain: no carbonatization and clay mineral replacement of primary mineralphases is observed, less LOI). Most of the main elements in relatively fresh samples from the central part (i.e., no. 5) do not show great variablilty. Smaller variabilities can be seen for MgO, K_20 (both positive) and Na_2O (negative).

For the AFT boulders (no. 8,9) a SiO_2, MnO, CaO, Na_2O depletion and a TiO_2, Al_2O_3, FeO, K_2O enrichment relative to the standard sample (no. 7) is observable (Text-Fig. 9). The ash tuffite (no. 1) follows the AFT boulder patterns at a lesser degree, except for P_2O_5, which is depleted relative to the standard.

The trace element variability for Rb, Sr, Y, Nb, Ba in relatively fresh samples from the central part (no. 5, 2 and 6) is rather large; only Cr, Zr contents show no variability (Text-Fig. 10).

The AFT boulders are enriched in Rb, Zr and Nb, depleted in Sr, Y and Ba. The ash tuff follows again the patterns of AFT boulders except in Y content, which is just a little outside the range of fresh samples.

Besides the described patterns it is nescessary to point to Appendix 2, which shows clearly a depletion of SiO_2, CaO, Na_2O and Sr and an enrichment of Al_2O_3, TiO_2, Fe_2O_3, K_2O and Rb from the central part to the

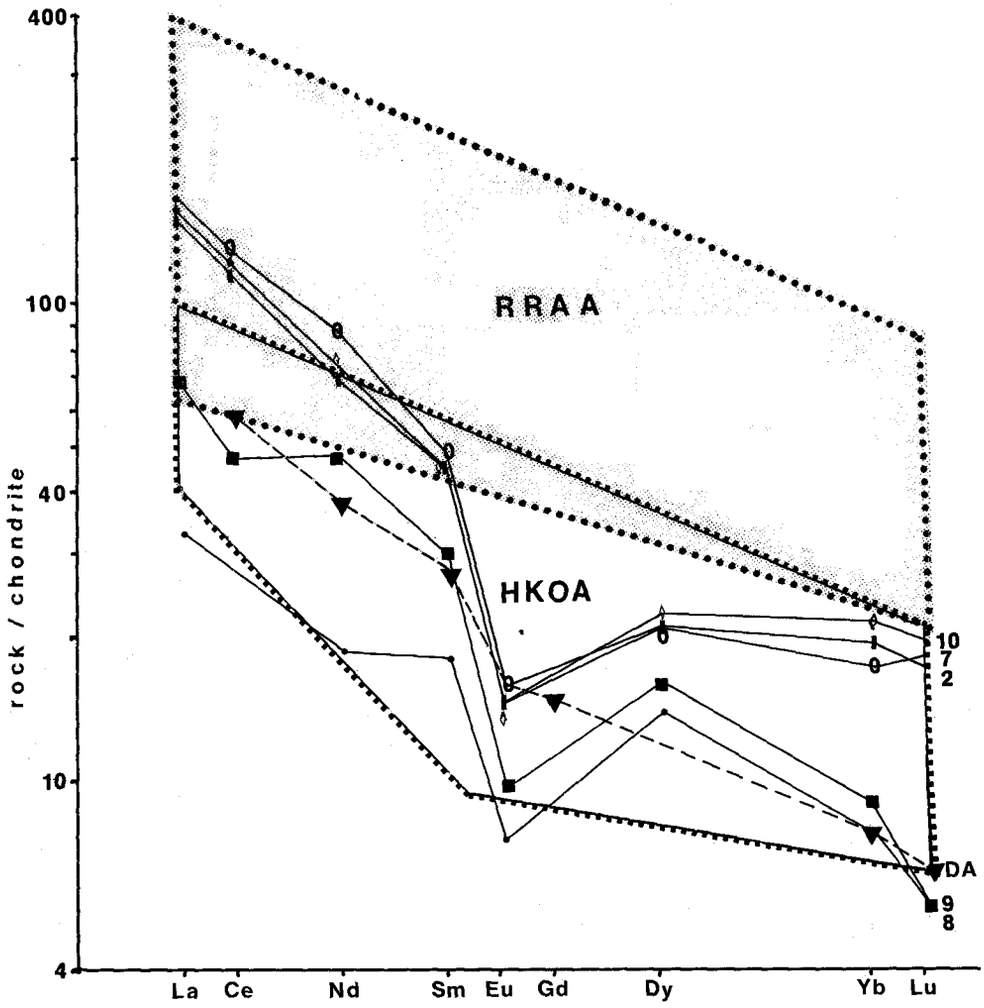

Text-Fig. 8.
Rock/chondrite diagram.
RRAA = Rift-related anorogenic andesites; HKOA = High-K orogenic andesites; DA = Dacite Andes.
For explanation see text.

top and to the base. Constant respectively in range of natural variation are MnO, P_2O_5, Cr Y, Nb and Ba.

The interpretation of these features cannot be summarized under one model, so we try to figure out what kind of processes could be responsible for the observed element distribution.

The enrichment of Al_2O_3, TiO_2 and Fe_2O_3 and the loss of SiO_2 indicates lateritic weathering conditions (H. GINSBERG, 1962). The paleoclimatic environment for the deposition of the Muschelkalk Conglomerate is determined as semiarid to arid, with periodically or seasonally high rates of precipitation (M. SCHMIDT, 1987). Such conditions would favour weathering. Also the genesis of palygorskite as a weathering product of basalts in this climate is well documented (M.K. HSNUDDIN SIDDIQUI, 1984). But compared with recent lateritic weathering sections of volcanic rocks a basal alteration is unknown.

The increase of K_2O and Rb, and the decrease of Na_2O, CaO and Sr, are more typical for hydrothermal alteration (C.D.A. SAWYER et al., 1989). But Zr, TiO_2 and other major elements should vary only slightly. Although we recognize such a pattern at the AFT and the enrichment of Zr, TiO_2, Al_2O_3 and Fe_2O_3 is probably caused by the loss of silica, we cannot accept this modell as it does not explain the loss of SiO_2.

Seawater alteration would strongly effect the less welded base and top of the AFT, as water/rock ratios in these parts are expected to be higher than in the central part (W.E. SEYFRIED & J.L. BISCHOFF, 1979; W.E. SEYFRIED & M.J. MOTTL, 1982). But neither low nor high temperature alteration can produce the pattern of the observed element mobility (i.e., the decrease of SiO_2 linked with the encrease of Al_2O_3).

Sample 14 was taken from the upper part of the AFT, but below the ash tuffite. In this part, cm-large areas consist of coarse grained calcite-quartz fabrics in which still relics of the AFT occur. The quartz contains a lot of very small fluid inclusions. Whether the precipitation of quartz and calcite is related to the loss of SiO_2 and CaO at the top and at the base of the AFT is not yet determined.

At the present state of research a two-stage alteration model is favoured. Lateritic weathering after deposition followed by hydrothermal and/or seawater alteration could produce the described element distribution of the core samples. The two AFT boulders are attached by this process at a higher degree than the massive deposit, indicating that other parts of the AFT are more altered than the core section or that the hand-sized boulders had been easier to convert. Small patches of quartz are ocurring in the carbonaceous groundmass surrounding the boulders of the conglomerate, possibly reflecting SiO_2 migration.

6. Discussion

6.1. Geochemical Results

In general there is little information in literature about Mesozoic ash-flow tuffs (C.S. ROSS & R.L. SMITH,

1961). So the petrography and geochemistry of the AFT document that the natural inhomogeneities caused by microxenoliths, alteration, or loss of fines during transportation do not show significant influences on bulk rock geochemistry of the central AFT. Main, trace and RE elements of the central AFT give us a clear element distribution of an "orogenic", calcalkaline magma.

The alteration patterns of the AFT, although not well explained untill now, are an important help to interpret other pyroclastic rocks of the Middle Triassic in the Southern Alps.

6.2. Plate Tectonic Setting

The geochemical composition of the AFT fits well with detailed studies of the massive lavas of the Southern Alps from Anisian to Carnian age. For the Karawanken Mountains (Austria) in the east (J.H. OBENHOLZNER, 1984, 1985; V. HÖCK & J.H. OBENHOLZNER, 1987) and for the Dolomites (northern Italy) in the southwest (A. CASTELLARIN et al., 1988) tectonic setting of basaltic to intermediate volcanics is interpretated to be island-arc related.

Recent results in igneous pertrology demonstrate that "orogenic", calcalkaline volcanics can also occur in intracontinental settings (D.G. BAILEY et al., 1989). These calcalkaline rocks are often associated with alkaline basalts, situated in an area of crustal extension. The author's investigations of basaltic rocks (Anisian–Ladinian) from the Carnic Alps (Italy), Dobratsch Mountain (Austria) and Orlica Mountains (Yugoslavia) suggest differentiation trends from mildly alkaline basalts to trachybasalts and to basaltic trachyandesites (J.H. OBENHOLZNER, unpubl. data).

The long known fact that an extensional tectonic regime created during Anisian and Ladinian times a facies differentiation according to basins and platforms, would support the hypothesis of an intracontinental magma genesis. The tectonic setting and the association of alkaline and "orogenic", calcalkaline rocks should initate a reinterpretation of the Middle Triassic magmatism to diminish the paleogeographical problems in the Southern Alps linked to the assumption of a subduction zone during the Triassic.

It is necessary to keep in mind that time equivalent features of compressional tectonics which do not confirm crustal extension are also observable (A. CASTELLARIN et al., 1985).

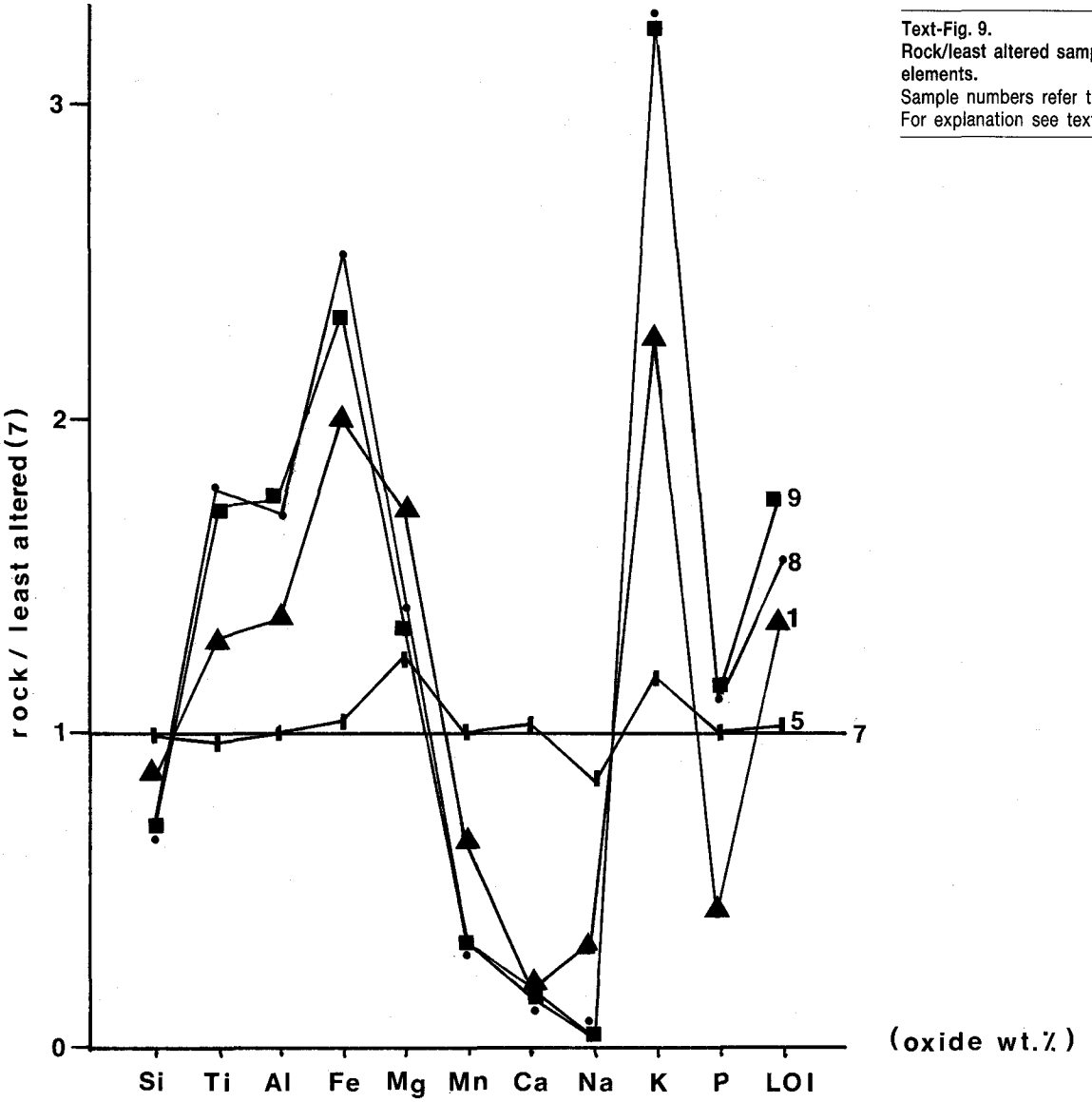

Text-Fig. 9.
Rock/least altered sample diagram for main elements.
Sample numbers refer to Table 3.
For explanation see text.

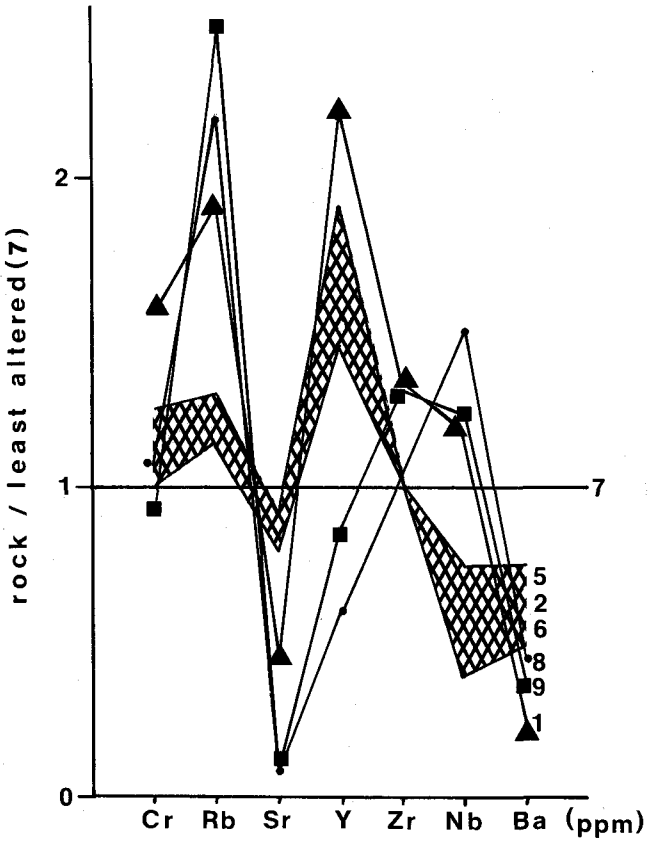

Text-Fig. 10.
Rock/least altered sample diagram for trace elements.
Sample numbers refer to Table 3.
Hatched area indicates variability for AFT samples 5, 2 and 6. For explanation see text.

6.3. Paleoenvironment

The fluvial deposition of the Muschelkalk Conglomerate is still under discussion (R. BRANDNER, pers. com.). For many volcanologists, ash-flow tuffs are an indicator for subaerial, explosive events. But S.R.J. SPARKS et al. (1980) demonstrated that welding could also occur under submarine conditions. So the AFT should not be used as an argument for fluvial or non-fluvial deposition of the Muschelkalk Conglomerate.

Acknowledgements

The author is grateful to Doz. Dr. H.P. SCHÖNLAUB and Dr. W. HOLSER for the opportunity to participate in the project and Dr. C.J. ORTH for analytical work. Thanks are also expressed to Prof. Dr. E. KIRCHNER (Institut für Geowissenschaften; Universität Salzburg) for clay mineral determination; G. NEUHUBER (Institut für Geowissenschaften; Universität Salzburg) for microprobe studies and Dr. W. HOLSER and Prof. Dr. W.J. SCHMIDT (Institut für Geowissenschaften; Montanuniversität Leoben) for critical reading of the manuscript.

Plate 1

Fig. 1: **White to greyish pumice fragment (P)**
with tubular (t) and ovoid - lensoid (o) vesicles - lithic fragment.
PPL .

Fig. 2: **Oxidized and slightly collapsed (small black arrows) pumice fragment**
with tubular vesicles - juvenile component.
Big black arrow points upward.
PPL .

Fig. 3: **Filled vacuole.**
Q = quartz; C = calcite.
The shape of the vacuole is outlined by iron oxides (thin dark rim); the AFT-matrix (M) is bleached around the vacuole.
PPL .

Fig. 4: **Typical shard texture of slightly to moderately welded central part of the AFT.**
Sampled at 31.5 m.
Shape of shards is shred-like; outlined by iron oxides. Shards consist of quartz and K-feldspar ± calcite.
Black arrow points upward.
PPL .

1 — 2 mm

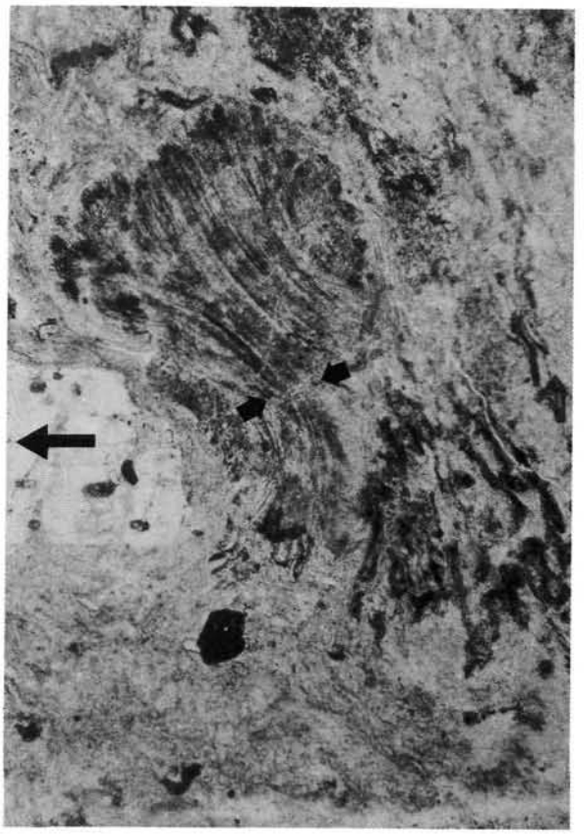

2 — 0,4 mm

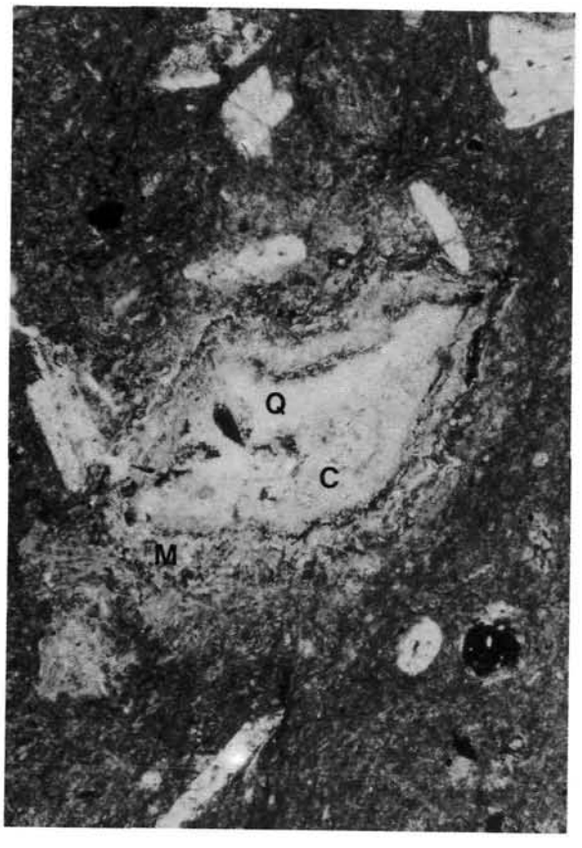

1 mm

4 — 0,4 mm

Plate 2

Fig. 1: **Basaltic–andesitic (?) lithic fragment,**
slightly rounded.
PPL .

Fig. 2: **Poikilitic plagioclase with inclusions of devitrified glass droplets.**
Alien (?) component. Embayed at middle; left side of the crystal.
PPL .

Fig. 3: **Crystal clot**
of plagioclases (P) with inclusion of apatite (A) needles and altered Ti-magnetite (T).
PPL .

Fig. 4: **Strongly embayed andesine (A).**
Deformation of AFT-matrix can be seen below plagioclase 1 and 2.
Black arrow points upward.
PPL .

1 mm

2

1 mm

3

1 mm

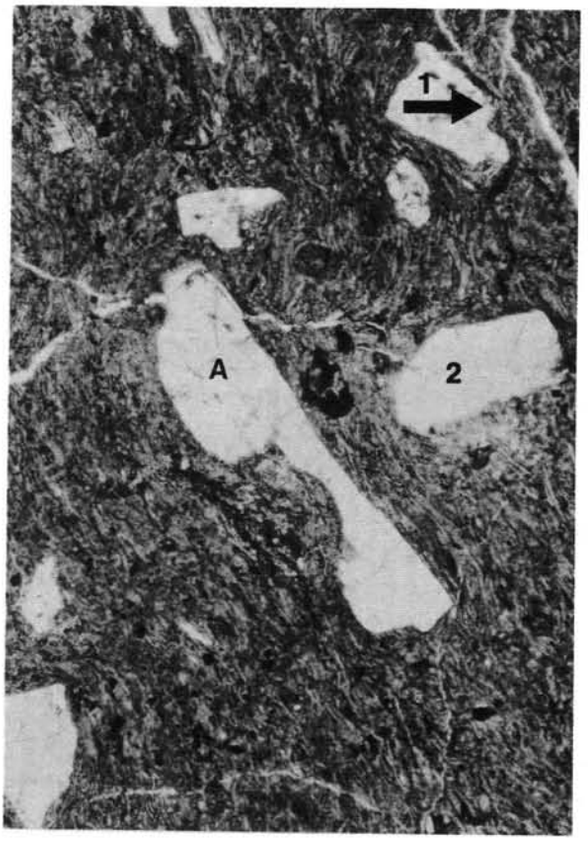

4

1 mm

References

BAILEY, D.G.: Calc-alkaline Volcanism Associated with Crustal Extension in Northeastern Oregon. – New Mex. Bureau of Mines & Mineral Res., Bull., **131**, p. 12, Socorro, 1989.

BEBIEN, J.: Magmatism Basiques Dits "Orogeniques" et "Anorogeniques" et Teneurs en TiO_2: Les Associations "Isotitanees" et "Anisotitanees". – J. Volcanol. Geotherm. Res., **8**, 337–342, 1980.

CAS, R.A.F. & WRIGHT, J.V.: Volcanic Successions, 528 S., London (Allen & Unwin) 1987.

CASTELLARIN, A., LUCCHINI, F., ROSSI, P.L., SELLI, L. SIMBOLI, G.: L'Evento Compressivo Medio-Triassico nelle Alpi Meridionali: Realita o Fantasia. – Mem. Soc. Geol. It., **30**, 235–44, Roma 1985.

CASTELLARIN, A., LUCCHINI, F., ROSSI, P.L., SELLI, L.& SIMBOLI, G.: The Middle Triassic magmatic-tectonic arc development in the Southern Alps. – Tectonophysics, **146**, 79–89, Amsterdam 1988.

CROS, P.: Decouverte d'Ignimbrites Anisiennes et Remaniement d'Ignimbrites Ladiniennes. Interpretation du Trias moyen des Alpes Carniques Orientales (Italie et Autriche). – C.R. Acad. Sc. Paris, **294**, ser.II, 911–914, Paris 1982.

DE VECCHI, G. & DE ZANCHE, V.: Potassium enrichment in Triassic volcanics. – N. Jb. Geol. Paläont. Mh., **10**, 573–579, 1982.

DUNGAN, M.A., THOMPSON, R.A., STORMER, J.S. & O'NEILL, J.M.: Rio Grande Rift Volcanism: Northeastern Jemez zone, New Mexico. – New Mex. Bureau of Mines & Mineral Res., Mem., **46**, 435–486, Socorro 1989.

EWART, A.: A review of the Mineralogy and Geochemistry of Tertiary–Recent Dacitic, Rhyolitic and Related Salic Volcanic Rocks. – In: BARKER, F. (ed.): Trondhjemites, Dacites and Related Rocks, 1979.

FARABEGOLI, E., JADOUL, F.& MARTINES, M.: Stratigrafia e Paleogeografia Anisiche delle Alpi Giulie Occidentali (Alpi Meridionali – Italia). – Riv. Ital. Paleont., **91**/2, 147–196, Milano 1985.

GILL, J.: Orogenic Andesites and Plate Tectonics. – 385 p., Springer Verlag 1981.

GINSBERG, H.: Aluminium. – 135 p., Stuttgart 1962.

HSNUDDIN SIDDIQUI, M.K.: Occurrence of Palygorskite in the Deccan Trap Formation in India. – In: SINGER, A., GALAN, E.: Palygorskite-Sepiolite-Occurrences, Genesis and Use. – Develop. in Sediment., **37**, 243–250, Amsterdam 1984.

HELLMAN, P.L., SMITH, R.E. & HENDERSON, P.: The Mobility of the REE: Evidence and Implications from Selected Terrains Affected by Burial Metamorphism. – Contrib. Mineral. Petrol., **71**, 23–44, 1979.

HÖCK, V. & OBENHOLZNER, J.H.: Triassic Magmatism in the Southern Alpine (Austria) . – Abstract in: Terra Cognita, **7**/2–3, p. 361, EUG IV, Paris 1987.

HORVATH E. & TARI, G.: Middle Triassic Volcanism in the Buda Mountains. – Annales Univ. Sci. Buda., Sect. Geol., **27**, 3–16, Budapest 1987.

HOWELLS, M.F., LEVERIDGE, B.E., ADDISON, R., EVANS, C. D. R. & NUTT, M.J.C.: The Capel Curig Volcanic Formation, Snowdonia, North Wales, Variations in Ash-Flow Tuffs Related to Emplacement Environment. – In: HARRIS, A.L., HOLLAND, L.H. & LEAKE, B.E. (ed.): The Caledonides of the British Isles; 611–618; Edinburgh 1979.

KAHLER, F. & PREY, S.: Erläuterungen zur Geologischen Karte des Naßfeld-Gartnerkofel-Gebietes in den Karnischen Alpen. – 116 S., Wien (Geol. B.-A.) 1963.

KOSHIMIZU, S.: Investigation of Pyroclastic Flow Deposits by Instrumental Neutron Activation Analysis (INAA). – Chem. Geol., **42**, 307–317, Amsterdam 1984.

LUCCHINI, F., ROSSI, P.-L., SIMBOLI, G. & VIEL, G.: Dati Petrografico della Serie Vulcanica Medio-Triassica dell' Area di Tarvisio (Carnia). – Miner. Petrogr. Acta, **21**, 135–150, Bologna 1980.

MIYASHIRO, A.: Volcanic Rock Series in Island Arcs and Active Continental Margins. – Am. J. Sci., **274**, 321–355, 1974.

NAKAMURA, N.: Determination of REE, Ba, Fe, Mg, Na, and K in Carbonaceous and Ordinary Chondrites. – Geochim. et Cosmochim. Acta, **38**, 757–775, 1974.

OBENHOLZNER, J.H.: Untersuchung der mitteltriadischen Vulkanite in den s.dalpinen Anteilen der Karawanken, Kärnten, Österreich. – Unpubl.Diss., Univ. Salzburg, 220 S., Salzburg 1984.

OBENHOLZNER, J.H.: Vorläufige Mitteilungen zur Petrographie und Geochemie mitteltriadischer Vulkanite im südalpinen Anteil der Karawanken (Kärnten, Österreich). – Arch. f. Lagerst.forsch. Geol. B.-A., **6**, 143–151, Wien (Geol. B.-A.) 1985.

PEARCE, J.A. & GALE, G.H.: Identification of Ore-Deposition from Trace-Element Geochemistry of Associated Igneous Rocks. – In: Volcanic Processes in Ore Genesis. Geol. Soc. London Publ., **7**, 14–24, London 1977.

ROSS, C.S. & SMITH, R.L.: Ash-flow tuffs: Their origin, geologic relations and identification. – U.S. Geol. Surv. Prof. Paper, **366**, 81 p., Washington 1961.

ROSSI, P.-L., RINALDI, R. & SIMBOLI, G.: Heterogeneous Feldspars in the Mid-Triassic Volcanis Rocks of the Dolomites. – Can. Mineral., **17**, 33–38, 1979.

SAWYER, D.A., SWEETKIND, D., RYE, R.O., SIEMS, D.F., REYNOLDS, R.L., ROSENBAUM, L.G., LIPMAN, P.W., BOYLAN, J.A., BARTON, P.B., BETHKE, P.M. & CURTIN, G.C.: Potassium Metasomatism in the Creede Mining District, San Juan Volcanic Field, Colorado. – New Mex. Bureau of Mines & Mineneral Res. Bull., **131**, p. 234, Socorro 1989.

SCHMIDT, M.: Sedimentologische und mikrofazielle Untersuchungen des Muschelkalkkonglomerates (Anis) im Gartnerkofel-Zielkofel-Gebiet (Karnische Alpen, Österreich). – Unpubl. Diplomarbeit, Universität Erlangen-Nürnberg, 102 S., Erlangen 1987.

SEYFRIED, W.E. & BISCHOFF, J.L.: Low Temperature Basalt Alteration by Seawater: an Experimental Study at 70°C and 150°C. – Geochimica et Cosmochimica Acta, **43**, 1937–1947, 1979.

SEYFRIED, W.E. & MOTTL, M.J.: Hydrothermal Alteration of Basalt by Seawater under Seawater-Dominated Conditions. – Geochimica et Cosmochimica Acta, **46**, 985–1002, 1982.

SPADEA, P.: Le Ignimbriti Riolitiche del Membro Superiore delle Vulcaniti di Rio Freddo, nel Trias Medio della Regione di Tarvisio (Alpe Giulie Occidentali). – St. Trentini WSc. Nat., A, **47**/2, 287–358, Trento 1970.

SPARKS, S.R.J., SIGURDSON, H. & WILSON, L.: Magma Mixing: a Mechanism for Triggering Acid Explosive Eruptions. – Nature, **267**, 315–318, 1977.

SPARKS, S.R.J., SIGURDSON, H. & CAREY, S.N.: The Entrance of Pyroclastic Flows into the Sea. II. Theoretical Considerations on Subaqueous Emplacement and Welding. – Jour. Volcanol. Geothermal Res., **7**, 97–105, Amsterdam 1980.

THORPE, R.S., POTTS, P.J. & FRANCIS, P.W.: Rare earth data and petrogenesis of andesite from the north Chilean Andes. – Contrib. Mineral. Petrol., **54**, 65–78, 1976.

WINCHESTER J.A. & FLOYD, P.A.: Geochemical Discrimination of Different Magma Series and their Differentiation Products Using Immobile Elements. –, Chem. Geol., **20**, 325–348, 1977.

WOOD, D.A., JORON, J.-L. & TREUIL, M.: A Re-appraisal of Trace Elements to Classify and Discriminate between Magma Series Erupted in Different Tectonic Settings. – Earth and Planet. Sci. Lett., **45**, 326–336, Amsterdam 1979.